

SCIENTIFIC REPORTS



OPEN

Ecosystem metabolism drives pH variability and modulates long-term ocean acidification in the Northeast Pacific coastal ocean

Alexander T. Lowe^{1,2}, Julia Bos³ & Jennifer Ruesink²

Ocean acidification poses serious threats to coastal ecosystem services, yet few empirical studies have investigated how local ecological processes may modulate global changes of pH from rising atmospheric CO₂. We quantified patterns of pH variability as a function of atmospheric CO₂ and local physical and biological processes at 83 sites over 25 years in the Salish Sea and two NE Pacific estuaries. Mean seawater pH decreased significantly at -0.009 ± 0.0005 pH yr⁻¹ (0.22 pH over 25 years), with spatially variable rates ranging up to 10 times greater than atmospheric CO₂-driven ocean acidification. Dissolved oxygen saturation (%DO) decreased by $-0.24 \pm 0.036\%$ yr⁻¹, with site-specific trends similar to pH. Mean pH shifted from <7.6 in winter to >8.0 in summer concomitant to the seasonal shift from heterotrophy (%DO < 100) to autotrophy (%DO > 100) and dramatic shifts in aragonite saturation state critical to shell-forming organisms (probability of undersaturation was >80% in winter, but <20% in summer). %DO overwhelmed the influence of atmospheric CO₂, temperature and salinity on pH across scales. Collectively, these observations provide evidence that local ecosystem processes modulate ocean acidification, and support the adoption of an ecosystem perspective to ocean acidification and multiple stressors in productive aquatic habitats.

Nearshore aquatic ecosystems are changing rapidly as a function of altered riverine inputs¹, eutrophication² and loss of foundation species due to human influence^{3,4}. Collectively these physical and ecological processes are changing carbon cycling, and interact with atmospheric CO₂ via warming and acidification to influence ecosystem function^{5,6}. While elevated aqueous CO₂, and the concomitant decrease of pH, has been shown to have negative effects across marine phyla⁷, the influence of long-term anthropogenic CO₂ emissions and the response of biological communities may vary by habitat in relation to local biotic and abiotic conditions^{8–10}. Microbial respiration has long been recognized as a driver of CO₂ exchange with the atmosphere along the aquatic continuum^{11,12}, particularly in net heterotrophic habitats such as shallow tidal estuaries and fjords that are typically sources of CO₂ to the atmosphere^{6,12}. Conversely, continental shelf and seasonally productive ecosystems can be CO₂ sinks¹³, suggesting a mechanistic link between local water chemistry and ecological factors such as interactions with organisms that modify the local environment, e.g. ecosystem engineers¹⁴, and food web dynamics¹⁵. While studies have shown that biological feedbacks have strong effects on carbonate chemistry on short time and small spatial scales^{16,17}, empirical studies investigating the potential for local ecological modulation of long-term global ocean acidification are lacking.

Currently, organisms are regularly exposed to ‘future’ levels of lower pH in nearshore ecosystems^{18,19}. The implications of these periods of low pH may depend on the timing of exposure²⁰, and go beyond the isolated physiological effects of pH when accompanied by multiple stressors like low oxygen or thermal stress²¹. But what controls these pH changes? Seawater pH has been demonstrated to respond to local community composition^{9,16,22} and changes to water column productivity or suspended particulate matter composition^{23,24} through the balance of primary productivity and respiration, referred to as net ecosystem metabolism. Few studies have paired quantification of ecosystem processes with pH, yet dissolved oxygen is commonly measured as an indicator of

¹Present address: Tennenbaum Marine Observatories Network, Smithsonian Institution, 647 Contees Wharf Road, Edgewater, MD, 21307, USA. ²Department of Biology, University of Washington, 24 Kincaid Hall, Seattle, WA, 98195, USA. ³Washington Department of Ecology, 300 Desmond Dr. SE, Lacey, WA, 98503, USA. Correspondence and requests for materials should be addressed to A.T.L. (email: lowea@si.edu)

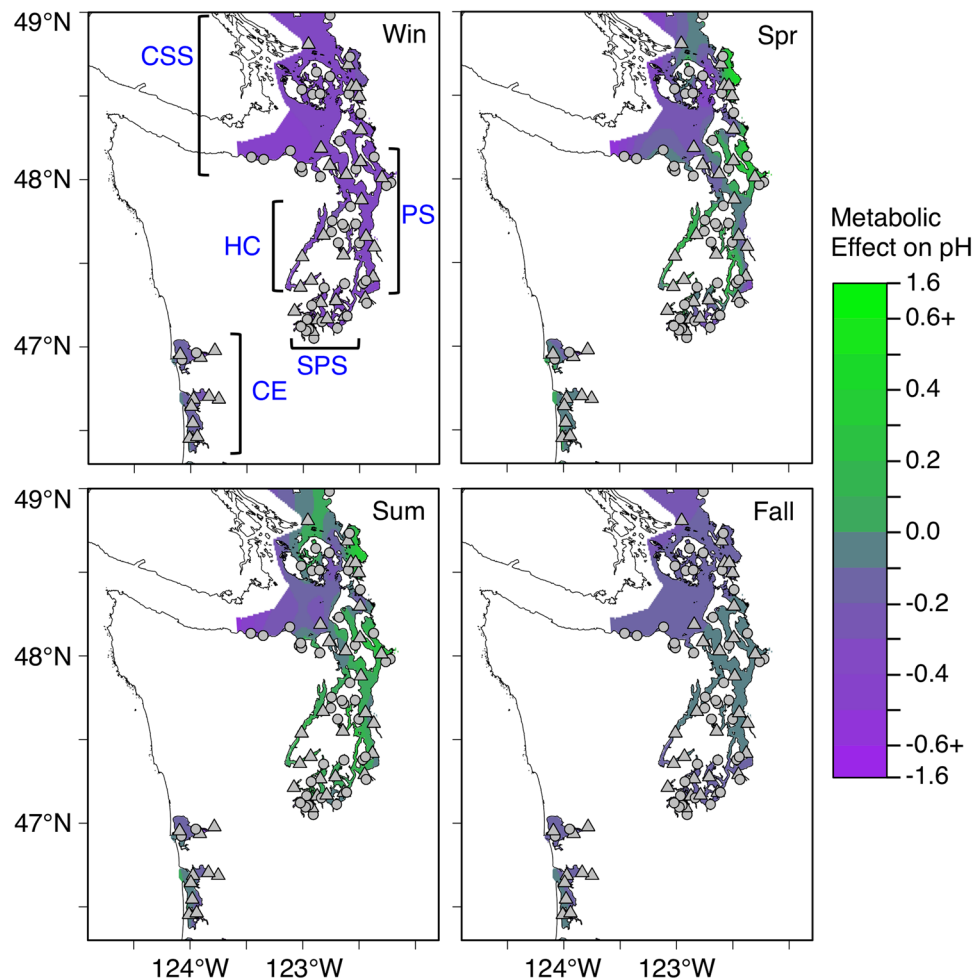


Figure 1. Seasonal mean metabolic effect on pH (observed pH minus predicted ‘atmospheric equilibrium’ pH) in Washington state waters, USA. Sampling location identified by dots (rotating) and triangles (core). Subregions defined in the analysis are coastal estuaries (CE), Hood Canal (HC), South Puget Sound (SPS), Puget Sound (PS) and Central Salish Sea (CSS).

net ecosystem metabolism²⁵. Long-term trends of pH that cannot be explained by increasing atmospheric CO₂ have been observed in coastal systems^{26,27} including long-term increases in mean pH^{8,28}. Empirical studies that compare trends in metabolic state and pH may fill this knowledge gap. The interaction of biological effects with water mass transport and physical processes could explain local variability of seawater pH on decadal¹⁰, annual²⁹ and monthly to hourly scales^{18,30}. Addressing ocean acidification from an integrated ecological framework may help define the temporal and spatial structure of exposure to pH stress and the relationship to other energetic and ecological factors at scales relevant to populations and communities³¹.

Previous studies have used long-term monitoring datasets to show that patterns of pH in shallow estuaries are closely linked to dissolved oxygen¹⁰ and to hypothesize that long-term pH changes in coastal shelf ecosystems are related to ecosystem productivity²⁸. In the current study, we quantified spatial and temporal seawater pH dynamics within a Northeast Pacific coastal region that includes upwelling-influenced shallow coastal estuaries, deep seasonally stratified fjord-like embayments, and tideflats. The diversity of habitats sampled in this study is representative of many seasonally productive coastal habitats around the world. We used monthly observations of water properties collected by U.S. state and federal agencies over 25 years to test the relative importance of hypothesized drivers of pH variability at 83 sites across ~7500 km² of coastal ecosystems in Washington state (Fig. 1). This region supports valuable wild and aquaculture shellfish industries that make up 45% of shellfish aquaculture in the US³² and may be vulnerable to long-term carbonate chemistry changes³³. We compared long-term trends of pH (NBS scale) to atmospheric CO₂ concentrations, then tested the hypotheses that global ocean acidification is modulated by local changes in net ecosystem metabolism as indicated by dissolved oxygen saturation. We then compared pH to physical and biological variables to test the relative importance of these variables at multiple timescales.

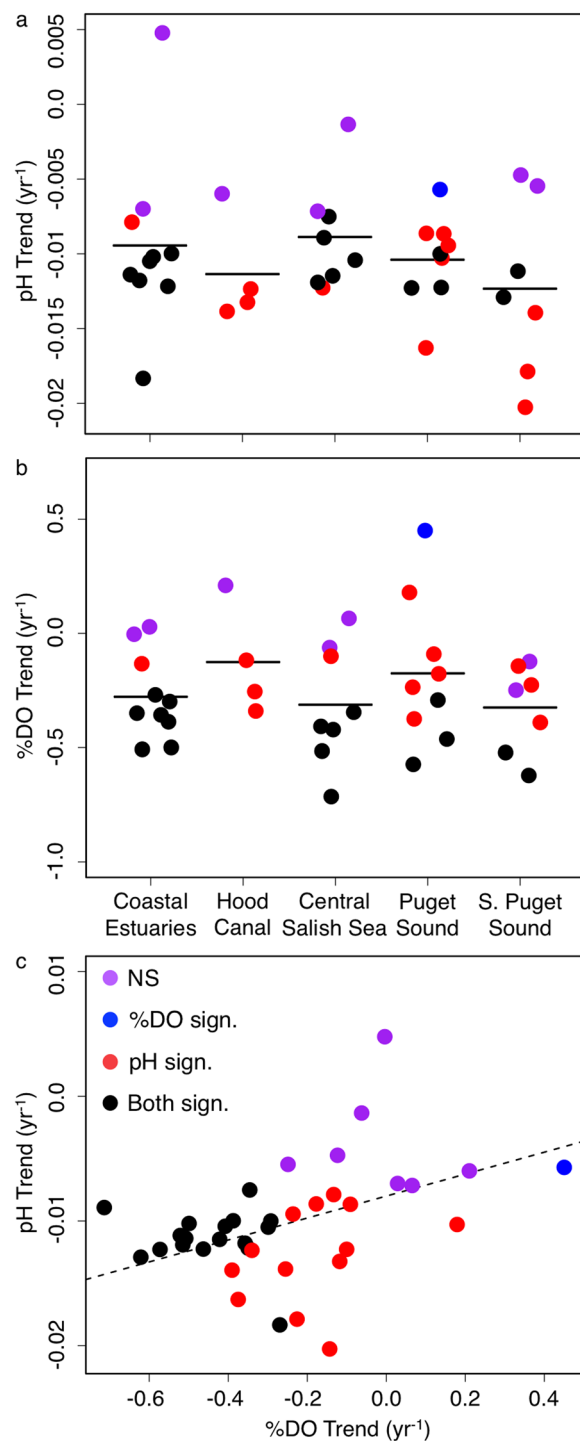


Figure 2. Calculated pH (a) and %DO (b) change per year for each subregion (horizontal bars) and individual core sites (points) from 1991–2015. Subregions for a and b shown below Fig. 2b. Site-specific trend of pH vs. trend of %DO (c). Dashed line is the slope of regression fit to all pH vs. %DO observations. Color of point indicates significance of trend: NS = neither pH or %DO trend over time were significantly different than zero at that site, DO Sign. = only %DO trend significant, pH Sign. = only pH trend significant, Both Sign. = both trends significant. Number of observations varies by site.

Results

Spatial and temporal variation of pH and %DO. *Multi-decadal pH and %DO trends.* Ecosystem-wide mean seawater pH decreased significantly during the period of sampling at a rate of -0.009 ± 0.0005 pH yr⁻¹ (LME: $X^2 = 331.5$, $df = 1$, $p < 0.001$). Estimates of mean pH trend showed little variation (-0.009 ± 0.0001 pH) associated with the method of subsampling data to unify datasets. Annual lower quartile pH declined significantly at -0.008 ± 0.003 pH yr⁻¹ over the sampling period (linear regression: $t_{1,23} = -2.78$, $r^2 = 0.22$, $p = 0.011$), whereas

	Obs.	Channel	Nearshore	Tideflat	System-wide
		2368	2042	1585	5995
Win	1066	7.61 ± 0.21	7.69 ± 0.23	7.80 ± 0.23	7.69 ± 0.23
Spr	1738	7.91 ± 0.29	8.00 ± 0.29	7.99 ± 0.31	7.96 ± 0.30
Sum	1766	8.03 ± 0.24	8.11 ± 0.25	7.94 ± 0.32	8.03 ± 0.27
Fall	1425	7.85 ± 0.22	7.93 ± 0.24	7.88 ± 0.27	7.89 ± 0.24
Annual	5995	7.88 ± 0.28	7.96 ± 0.30	7.91 ± 0.30	7.92 ± 0.29

Table 1. Summary of mean and standard deviation of pH observations by season and habitat. Number of observations in each category shown in table.

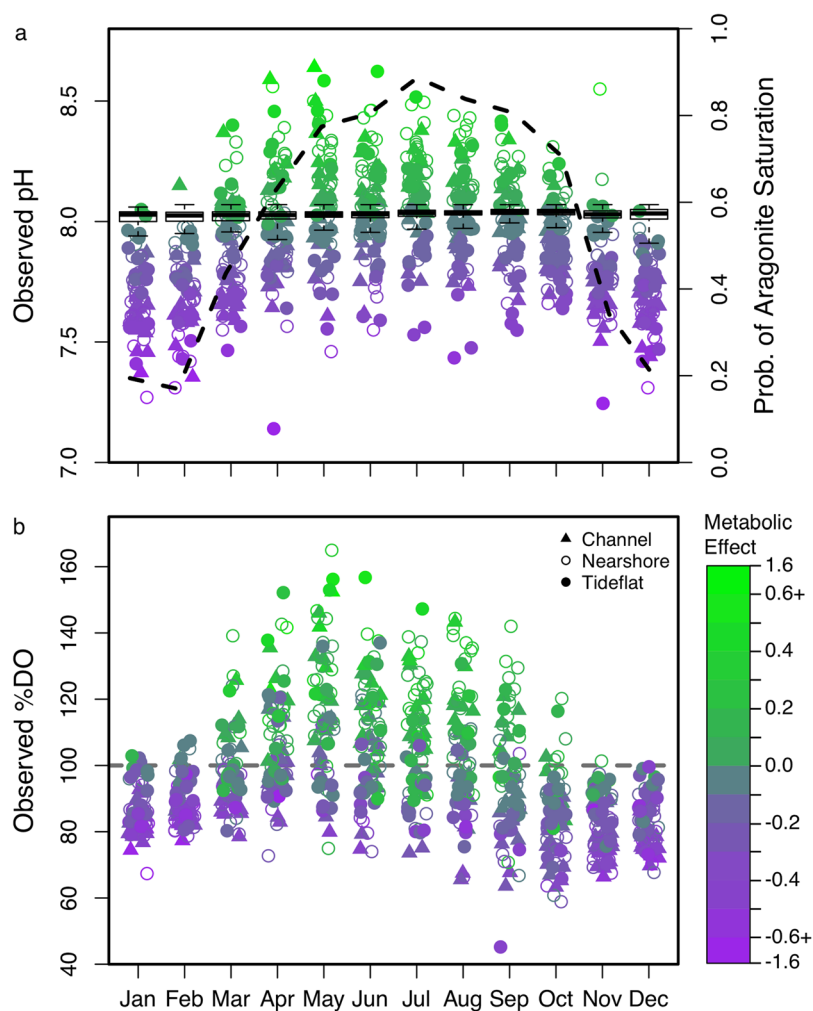


Figure 3. Seasonal variation of observed pH and %DO. (a) Mean monthly site-specific pH (points), distribution of predicted 'atmospheric equilibrium' pH across all sites for each month (boxplots), and the probability of observing aragonite supersaturation within the entire sampling region in a given month (dashed line corresponding to right axis). (b) Mean monthly site-specific dissolved oxygen saturation. Color of points in a and b corresponds to the magnitude of the metabolic effect on pH (observed pH minus 'atmospheric equilibrium' pH) as indicated in the legend (same as Fig. 1). Shape of points indicates habitat of the site: triangle = channel, open circle = nearshore, filled circle = tideflat.

annual upper quartile pH did not change over the period (linear regression: $t_{1,23} = -0.75$, $r^2 = 0.023$, $p = 0.459$). The mean pH decreased significantly at 30 of 38 core sites at rates ranging from -0.008 to -0.020 pH yr^{-1} (Fig. 2a). The mean rate of pH change varied by subregion, and was greatest in South Puget Sound. %DO decreased in the region by $-0.24 \pm 0.036\%$ yr^{-1} (LME: $X^2 = 42.2$, $df = 1$, $p < 0.001$). Significant negative trends were observed at 17 of 38 core sites and ranged from -0.27 to -0.71% yr^{-1} , with one significant positive trend of $+0.45\%$ yr^{-1} (Fig. 2b). Site-specific trends of pH and %DO were similar to the expected relationship derived from

Variable	pH			%DO		
	Df	F	p	Df	F	p
Site	82	25.30	<0.001	82	30.46	<0.001
Month	11	216.10	<0.001	11	311.87	<0.001
Site*Month	794	2.09	<0.001	794	2.95	<0.001
Residuals	5107			5107		
Subregion	4	44.05	<0.001	4	65.33	<0.001
Season	3	419.91	<0.001	3	560.59	<0.001
Subregion*Season	12	27.62	<0.001	12	40.04	<0.001
Residuals	5975			5975		
Habitat	2	47.67	<0.001	2	52.28	<0.001
Season	3	409.76	<0.001	3	516.96	<0.001
Habitat*Season	6	27.93	<0.001	6	28.44	<0.001
Residuals	5983			5983		

Table 2. Results of linear models comparing pH and %DO across spatial and temporal scales.

	Estimate	SE	X ²	p
DO % Saturation	0.595	0.010	2672.30	<0.001
Atmosphere CO ₂	-0.201	0.009	507.86	<0.001
Temperature	0.184	0.014	157.62	<0.001
Salinity	0.030	0.010	7.94	0.005

Table 3. Results of linear mixed effects model comparing pH variation to metabolic (%DO), physical (temperature and salinity) and climatic (atmospheric CO₂) drivers. (see methods for details, briefly: LME model with 5994 observations scaled to (x-μ)/SD for each variable. Fixed effects shown, random effects were Subregion and Season.

the regression of pH to %DO (Fig. 2c; slope = 0.008), but deviations at multiple sites lead to a non-significant relationship between the trends.

Seasonal and spatial variability of pH and %DO. Overall, mean daytime pH was 7.92 ± 0.30 in Washington State surface waters during the period from 1991 to 2015 (Table 1). Average %DO was $97.8 \pm 21.5\%$. The probability of observing aragonite supersaturation ($\Omega > 1$) shifted from <20% in winter to 88% in July (Fig. 3a), concomitant to a system-wide shift from net heterotrophy (%DO < 100%) to autotrophy (%DO > 100%). The seasonal oscillation of median pH was robust enough to be observed even though mean pH decreased by ~0.22 units over the period of sampling. Metabolic contribution to pH varied considerably among sites and seasons (Fig. 1), leading to a range of pH as much as 1.3 units above and below predicted atmospheric equilibrium. These changes were much greater than could be explained by physical factors alone (black boxplots show distribution of 'atmospheric equilibrium' pH; Fig. 3a). In total, only 6.6% of observations over 25 years were within one standard deviation of the mean 'atmospheric equilibrium' seawater pH.

Significant spatial and temporal variation of mean pH and %DO was observed at multiple scales (Table 2); pH and %DO varied significantly among sites and months (Fig. 3), as well as at the subregional and seasonal scale (Table 2). Habitat was also a significant predictor of pH and %DO (Table 2; Fig. 3). The pH at channel and nearshore sites exhibited high variation among seasons, on average ranging 0.43 pH from summer to winter in channel and 0.42 pH in nearshore sites (Table 1). Tidel flats exhibited high pH variation within seasons, particularly in summer and fall when variation was ~30% and 17% higher, respectively, than channel and nearshore habitats (Bartlett's test: Summer, $K^2 = 56.4$, $p < 0.001$; Fall, $K^2 = 18.3$, $p < 0.001$; Table 1). Seasonal variation over the year was largely due to changes in the maximum observed pH, which varied >1.2 pH from winter to summer, rather than a change in the minimum observed pH which varied ~0.3 pH over the year. %DO exhibited a similar pattern (Fig. 3b)

Time of day. Surface pH increased 0.026 ± 0.001 pH hr⁻¹ (LME: $X^2 = 250.41$, $df = 1$, $p < 0.001$) and %DO increased $1.54 \pm 0.010\%$ hr⁻¹ (LME: $X^2 = 132.4$, $df = 1$, $p < 0.001$) during the daytime sampling period when controlling for interannual and subregional differences.

Drivers of pH variability. pH was significantly positively correlated to dissolved oxygen, temperature and salinity, whereas pH was significantly negatively correlated to atmospheric CO₂ (Table 3). The scaled estimate of %DO influence on pH was nearly three times larger than the effect of temperature (0.595 vs. 0.184) and an order of magnitude greater than the effect of salinity (0.030). The effect of atmospheric CO₂ was of similar magnitude but opposite sign as temperature (-0.201). %DO alone explained 50.9% of the variation in pH, whereas the

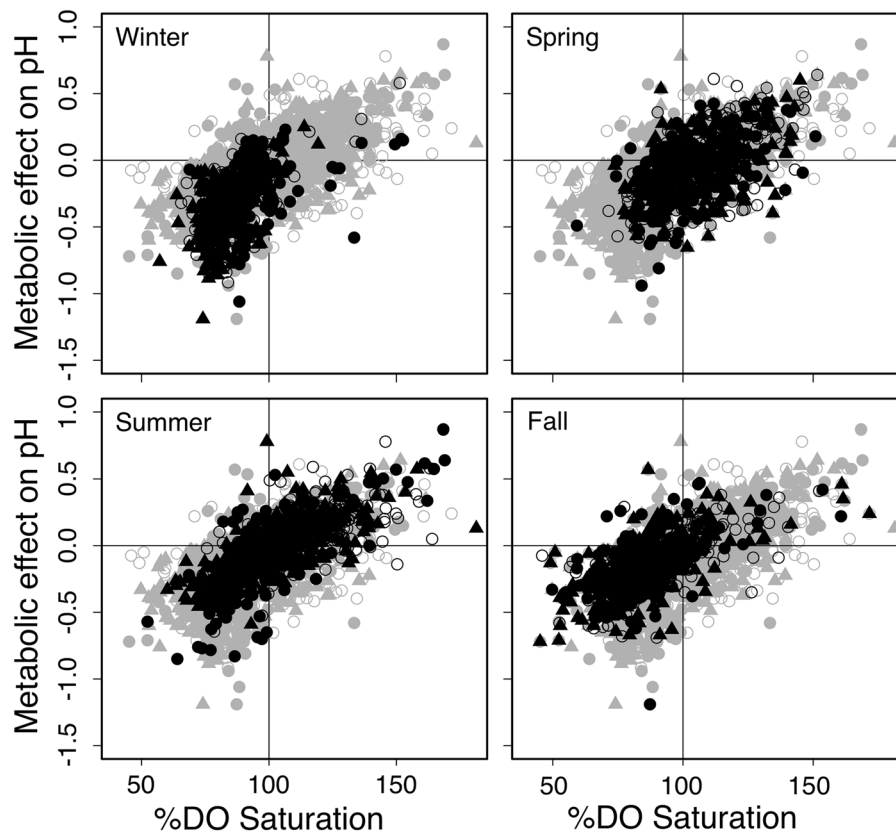


Figure 4. Relationship of mean seasonal metabolic effect on pH vs. %DO saturation. Crossbars indicate 'atmospheric equilibrium' pH and 100% DO saturation. Black points represent the seasonal site-specific mean pH across all years of sampling. Light gray points show all values. Shape of points indicate habitat: triangle = channel, open circle = nearshore, filled circle = tideflat.

full model including temperature, salinity and atmospheric CO_2 explained 54.8%. Chlorophyll was positively correlated to pH in the subset of data with chlorophyll measurements (Supplementary Table 2). The relationship between pH and DO varied slightly by season (Fig. 4); the slope of the regression of pH anomaly to %DO was 0.011 in winter ($r^2 = 0.27$, $p < 0.001$), 0.008 during spring ($r^2 = 0.28$, $p < 0.001$), 0.009 in summer ($r^2 = 0.51$, $p < 0.001$) and 0.008 in fall ($r^2 = 0.39$, $p < 0.001$). Both DO and pH were predominately lower than atmospheric equilibrium in fall and winter, with a large shift towards positive pH anomalies and DO supersaturation occurring in spring and summer (Fig. 4).

Discussion

Multi-decadal changes of surface water pH have been observed in marine ecosystems^{34,35} yet few datasets have quantified the parameters necessary to test hypotheses about the potential for biological processes to modulate pH changes over time (but see¹⁰). We quantified the effects of atmospheric CO_2 , physical and biological factors on seawater pH using a unique dataset spanning 25 years of sampling at 83 sites representing shallow estuarine, nearshore, and deep, stratified coastal habitats. Surface seawater pH decreased significantly over the 25-year study period in this NE Pacific coastal ecosystem. While pH was negatively correlated to atmospheric CO_2 , the rate of pH decrease was on average ~5 times greater than that predicted from atmospheric CO_2 changes alone. Concomitant changes to dissolved oxygen support the hypothesis that local biological processes modulated global ocean acidification, in this case accelerating long-term pH decline. Multiple lines of evidence support the hypothesis that changes to local ecosystem metabolism and a system-wide shift towards greater net heterotrophy, more than physical oceanographic conditions or atmospheric CO_2 , caused the rapid decline of pH. First, the ecosystem-wide trend of $-0.009 \text{ pH yr}^{-1}$ corresponded to deoxygenation at a rate of $-0.24\% \text{ yr}^{-1}$. Second, the rate of pH and %DO were non-uniform among sites within the same ecosystem, with significant pH decreases ranging from 4–10 times that of open ocean rates of acidification. Third, this system was on average a source of CO_2 to the atmosphere and pH was within one standard deviation of atmospheric equilibrium only ~6% of the time. Fourth, %DO explained a majority of variation in pH across scales, including coherent seasonal variation across the region and observable increases associated with the time of day samples were collected. Finally, the significant long-term decline of pH was driven by changes to the lower quartile of pH from an intensification of heterotrophic conditions with no corresponding change to the upper quartile range, contrary to model predictions driven by atmospheric changes¹⁷. Collectively, these observations implicate local ecosystem metabolism

as the main driver of variation of pH in NE Pacific coastal habitats. The diversity of habitats represented in this analysis indicates these findings are generalizable to many coastal ecosystems.

This empirical analysis of long-term pH and oxygen changes revealed a primary influence of net ecosystem metabolism on pH dynamics. Biological community composition has been observed to influence carbonate chemistry variation in tide pools and coral reef flats^{9,16}; we provide evidence that strong biological influence can extend to an ecosystem-scale. The extremes of pH ($6.5 < \text{pH} < 9.3$) were far outside the range driven by physical changes alone and were correlated to extremes of %DO. The widespread prevalence of respiration-driven undersaturation of surface waters in fall and winter means organisms are regularly exposed to stressful carbonate chemistry conditions as a function of the seasonal cycle of biomass production and decomposition. Yet as %DO increased seasonally, aragonite saturation state shifted from levels stressful to local organisms^{7,36,37} to benign conditions. The shift towards benign conditions corresponded to the timing of sensitive early life history stages in many organisms³⁸, suggesting these seasonal fluctuations may have considerable consequences for populations of aquatic organisms. The system-wide, biologically-driven shift towards higher pH in summer is likely an important feature of seasonally productive nearshore ecosystems.

The observed habitat-specific pH dynamics lend further support for the importance of considering ecological processes in ocean acidification studies, and the need for studies parsing variability among benthic and pelagic factors. High macrophyte biomass, often cited as a potential acidification refuge³⁹, may have contributed to elevated pH in tidelflat habitats, particularly in eelgrass-dominated areas of PB-NERR (Central Salish Sea) and Willapa Bay (Coastal Estuaries). Macrophyte production can exert large positive effects on pH in shallow coastal habitats^{10,39,40}, but could not explain elevated pH observed in nearshore (>20 m depth) and channel habitats (>60 m depth) throughout much of the spring and summer (Fig. 3). Phytoplankton blooms can lead to increased pH^{13,41} particularly in stratified systems like Puget Sound and Hood Canal⁴² in which the effect of primary productivity may be magnified by spatially decoupled productivity and decomposition^{23,43}. Nearshore and channel habitats that experience seasonal stratification had elevated and less variable pH during spring and summer compared to well mixed areas like the coastal estuaries and sites within the Central Salish Sea (Fig. 1). The correlation of pH to chlorophyll and %DO concentration provides further evidence that distributed microalgae are ecosystem engineers of carbonate chemistry at large scales, a suggestion corroborated by observations of a transition from aragonite undersaturation to supersaturation concomitant to seasonally elevated primary productivity from numerous locations, including the West Antarctic Peninsula⁴⁴, North Atlantic¹³, western Arctic Ocean²³, Dutch Coastal zone²⁸, the St. Lawrence Estuary⁴⁵ and the Busan coast in South Korea⁴⁶.

Quantifying connections to broader oceanographic processes is important to predict patterns of local pH variation⁴⁷. Seasonal upwelling, freshwater inputs from rivers, and temperature changes putatively drive variation of carbonate chemistry in many coastal systems^{48,49}. The influence of upwelling in Washington's coastal estuaries dissipates quickly with distance into the bay as biological processes begin to modulate variability³⁰. Patterns of pH variation consistent with the influence of upwelling were not observed on a large scale in this study; instead, pH patterns were more parsimoniously related to diel, seasonal and habitat-driven changes in ecosystem metabolism. Freshwater reduces seawater buffering capacity, which should result in lower pH¹. Weak negative effects of decreased salinity on pH were observed, and may be localized in coastal ecosystems of NE Pacific Ocean, for example, contributing to the low mean pH observed in the Coastal Estuaries in this study. The observations of salinity <15 that were excluded from this analysis represented ~6% of the dataset, primarily in the Coastal Estuaries; the overall small relative effect of salinity is representative of the biologically-driven pH variation in this system. Negative effect of decreased salinity may also be counteracted by indirect effects of freshwater input on density stratification that result in increased primary productivity²⁴. Contrary to predictions based on physical changes alone, temperature was positively correlated to pH, even when controlling for seasonal and subregional differences. However, this positive correlation was not evident at temperatures greater than ~18 °C. The transition to heterotrophy at peak summer temperatures has been observed to drive pH and %DO decreases in many estuaries^{10,25} and highlights the importance of considering the interaction of abiotic and biotic factors across scales. The small physical effects compared to the effect of ecosystem metabolism suggests that oceanographic control of carbonate chemistry in this ecosystem is indirect, and largely a function of physical effects on primary productivity and respiration.

Studies in the open ocean have observed spatial variability in long-term trends of pH, but the trends generally correspond to increased atmospheric CO₂^{34,50}. We documented variable rates of pH change among sites within a single ecosystem that ranged up to 10 times greater than the atmospheric CO₂ trend. Furthermore, many sites had non-significant negative trends and one site in Willapa Bay within the Coastal Estuaries had a positive, but non-significant, trend of pH (Fig. 2a). High variability in the rate of pH change among sites within the same ecosystem, and even within the same subregion, provides strong evidence for local ecosystem drivers of pH fluctuations^{8,10,27,28}. High spatial variability, particularly over tidelflats, suggests models based on mid-channel monitoring may inaccurately predict conditions on the benthos due to different ecological contexts. Across sites, decadal-scale decreases of %DO and increasing heterotrophy are further support a biological driver of declining pH. The long-term pH and %DO trends generally fell along the expected relationship between pH and %DO, but some sites deviated from this pattern (Fig. 2c). Deviations may be driven by methodological factors such as years of sampling or physical variables such as the diffusion rates of pH and %DO at extremes of the observed range. Oxygen and CO₂ solubility differ by an order of magnitude, a factor that may be important in surface waters with large deviations from atmospheric equilibrium of pH (e.g. ± 1.3 pH) and DO (30–200% saturation) driven by biological processes⁵¹. These extremes lead to dramatic gradients in air-sea gas concentrations that could explain poor correlation between pH and DO at sites with high variability of these parameters⁵².

Ecological factors like the spatial coupling or de-coupling of biomass production and decomposition can furthermore play a large role in the observed relationship between pH and dissolved oxygen, particularly in high productivity, stratified nearshore regions. The theoretical relationship between primary production and

respiration may not accurately predict empirical observations, particularly at longer timescales when variable rates of gas exchange and mixing water masses alter effects of local biological processes¹⁰. The movement and mixing of water masses can contribute to decoupling of biomass production and decomposition, leading to poor correlation between local pH and %DO. Much of this region experiences large tidal exchanges (>3 meters), seasonal wind-driven mixing and estuarine circulation such that measurements taken at monthly intervals may encounter water masses with different histories. Long-term monitoring programs are critical for establishing baselines and identifying anomalies of exposure to pH and dissolved oxygen. This study provides evidence that the seasonal changes to local ecosystem metabolism dominate other sources of variability in this system, but more research at different scales is required to fully understand the influence of physical and biological factors on pH dynamics across ecosystems.

The atmospheric equilibrium model of ocean acidification was inadequate for predicting recent (25-year) changes in this productive nearshore ecosystem: surface water was net heterotrophic over the study period and rarely in equilibrium with the atmosphere. Predicting exposure of marine organisms to stressful carbonate chemistry cannot exclusively follow global-scale biogeochemistry trends and will be improved through integration of organisms as drivers, not just responders, of change. Acknowledging the biological influence on pH variability allowed us to link ecologically-driven pH changes to temporal and spatial heterogeneity of CO₂ exchange with the atmosphere in response to net organic matter production (Fig. 1, estimated CO₂ sink = green) and decomposition (Fig. 1, CO₂ source = purple)⁵³. This framework provides the basis for integrating studies of physiological, community, and food web ecology with biogeochemical studies⁵⁴. Many food webs in coastal habitats include reciprocal linkages from the water column to the benthos, particularly when phytoplankton serve as food to suspension-feeders but may compete for light with macrophytes. The quality and quantity of suspended particles derives in part from the balance of phytoplankton production and decomposition, and these suspended particles in turn influence turbidity, light penetration, and food quality for suspension feeders. High concentrations of detrital particulates in the water column simultaneously limit light penetration and subsequent photosynthetic uptake of CO₂ by macrophytes¹¹, while contributing CO₂ from microbial degradation of detrital particulates⁵³. The sensitivity of pH to net ecosystem metabolism suggests that the growing network of pH sensors around the world contributes to monitoring long-term pH changes, while providing an unprecedented ability to observe ecosystem function in near-real time and improve the resolution of carbon flux dynamics from a diversity of habitats, a biogeochemical research priority⁵⁵. The diversity of nearshore habitats covered by our study adds to those such as riverine¹, salt marsh⁵⁶, shallow estuarine systems^{53,57} and tidepools¹⁶ in which ecosystem metabolism modulates local pH variability and response to global climate change.

Materials and Methods

Spatial and temporal variation of pH and %DO. Patterns of seawater pH (NBS scale) and the relationship to abiotic and biotic ecological factors were quantified in the coastal waters of Washington State at 83 sites spanning 25 years from 1991–2015 (Fig. 1). Sites were distributed throughout five subregions including the Coastal Estuaries (Grays Harbor and Willapa Bay), Hood Canal, South Puget Sound (south of the Tacoma Narrows), Puget Sound (main basin and Whidbey basin) and Central Salish Sea (sites north of Admiralty Inlet and in eastern Strait of Juan de Fuca). Environmental data were collected by the Washington state Department of Ecology (80 sites, WA-DOE) (fortress.wa.gov/ecy/eap/marinewq/mwdataset.asp) and the Padilla Bay National Estuarine Research Reserve (3 sites in Central Salish Sea, PB-NERR) (cdmo.baruch.sc.edu/get/export.cfm). Data used in this analysis met rigorous calibration and quality control standards. Data from WA-DOE include monthly water column profiles sampled at 0.5 m depth increments spanning the time period from October 1991 – October 2015⁵⁸. Temperature (°C), salinity, dissolved oxygen (DO, mg L⁻¹, % saturation) and pH (NBS scale) data were measured with SBE sensors (Sea-Bird Electronics, Inc.) throughout the study period. WA-DOE monitors 38 permanent ‘core’ sites and 45 rotating sites; all data were used for seasonal summaries and modeling analyses, whereas long-term trends were assessed with core sites owing to longer periods of observation. PB-NERR data were collected from moored, stationary sensors at 30 min (1995–2007) or 15 min (2007 – October 2015) intervals. Temperature (°C), salinity, dissolved oxygen (DO, mg L⁻¹, % saturation) and pH (NBS scale) data were measured using an YSI 6600 multiprobe sonde (YSI, Inc.). These three sites were included in the ‘core’ sites for long-term analyses.

The methods of data collection differed in that a single time point was associated with multiple depths at WA-DOE sites, but only a single depth at PB-NERR sites. To make observations from these datasets comparable, one observation representing a single time and depth was randomly selected for each month from the 304,989 observations from the WA-DOE and PB-NERR monitoring sites resulting in 5994 observations. For PB-NERR sites, the monthly sample was selected during daytime hours between 0900 and 1700 local time. For WA-DOE sites, one measurement near the surface of each monthly depth profile (0.5 to 4.5 m) was selected at random. Observations were filtered to exclude measurements of salinity <15 to restrict error associated with predicting carbonate chemistry parameters below this level⁵⁹. The subsampling method provided a data set with appropriate weighting (one sample per site and month each year) but used a small fraction of the data. To ensure the random sample used in the following analyses gave robust results and were not biased by the subsampling method, we compared long-term trends of pH and dissolved oxygen calculated with independent subsamples of the full ‘core’ site dataset (250 iterations).

Multi-decadal pH and %DO trends. Long-term temporal trends over the 25-year study period were assessed for both pH and %DO saturation with data from the 38 core sites (N = 4961 observations) using a linear mixed-effects model structure (LME) with year as explanatory factor and subregion and season as random effects. These smaller-scale factors were considered random effects here, where the focus was on long-term trends, but were explicitly considered for their contributions to pH variability in subsequent analyses (see below). Separate

linear regressions were run for the upper-quartile and lower-quartile of the annual pH distribution. In addition to the region-wide analysis, trends at each core site were assessed separately using linear models. Not all sites were sampled in every month.

Seasonal and spatial variability of pH and %DO. Patterns of variability of mean pH and %DO were investigated using linear models with multiple spatial (site, habitat, subregion) and temporal scales as predictor variables. Habitats included tide flat (22 sites; <~17 m depth, sampled over tidal flat or predominantly well-mixed shallow inlets influenced by tidal flats), nearshore (38 sites; water depth was 17–60 m and close to shore or within a confined embayment) and channel (23 sites; in main channels with water depth >60 m). Homogeneity of variance of pH among habitats was tested in each season using Bartlett's test. Seasons were defined as Winter = December, January, February, Spring = March, April, May, Summer = June, July, August, and Fall = September, October, and November.

In addition to this statistical modeling, the extent to which surface waters in the region were out of equilibrium with the atmosphere was visualized by developing a metric to demonstrate the metabolic effect on pH, analogous to %DO. Metabolic effect on pH was calculated by subtracting the predicted 'atmospheric equilibrium' pH based on physical conditions from the observed pH. 'Atmospheric equilibrium' pH was calculated using local temperature, salinity, estimated alkalinity from salinity *sensu* ⁽⁶⁰⁾ and *p*CO₂ in the 'seacarb' package in R⁵⁹. We assumed that *p*CO₂ concentration was in equilibrium with the mean annual atmospheric concentration obtained from NOAA (www.esrl.noaa.gov/gmd/ccgg/trends/). The marine source water that feeds Puget Sound and Hood Canal is characterized by mean *p*CO₂ concentration near 700 μatm⁶¹. Source water for the Coastal Estuaries may include upwelled deep North Pacific water³⁰. Seasonal variation of the source water to these subregions is difficult to constrain because of limited observations. We therefore used atmospheric CO₂ concentration as the equilibrium point for the calculation of the metabolic effect because (a) most ocean acidification model projections consider surface oceans to be in equilibrium with the atmosphere, (b) surface waters of this region are in contact with the atmosphere for timescales required to reach equilibration with the atmosphere⁶², (c) this assumption simplifies the treatment of different water bodies that vary in their marine and freshwater sources, and (d) comparing *p*CO₂ to atmospheric CO₂ allows for a simple indicator of source-sink dynamics. Using the mean Strait of Juan de Fuca water (~7.8) as the equilibrium point would not effect the analyses in this paper, it would simply amplify pH anomalies by ~+0.2 units without changing seasonal patterns. The predicted pH was subtracted from the observed pH so that positive deviations (CO₂ sink) indicate the influence of primary productivity while negative deviations (CO₂ source) indicate the influence of respiration either locally or transported from outside the system.

To investigate potential consequences of pH variation for calcifying organisms, aragonite saturation state was calculated in 'seacarb' with observed pH, temperature, salinity and alkalinity predicted from salinity. The proportion of observations above saturation ($\Omega > 1$) was calculated for each month. The probability of saturation metric is a conservative estimate of stressful carbonate chemistry conditions as organisms have been observed to be sensitive to aragonite saturation states of <1.6³⁶, and states <1 mark the physical threshold of aragonite dissolution.

Time of day. Small-scale (within-day) temporal variability of pH and %DO associated with time of sampling was quantified using linear mixed effects models with random effects of site and season within year (N = 5994).

Drivers of pH variability. Analyses and visualizations described in prior sections tested for spatial and temporal variation of pH and %DO at different scales. Here, %DO is incorporated as a potential predictor of pH, along with abiotic and climatic factors considered likely drivers. Subregion and season were identified as random effects following methods in⁶³ to constrain spatial and temporal variation. Explanatory variables that were correlated to each other ($r > 0.6$) were excluded from the same analysis. Temperature, salinity and %DO data sampled simultaneous to pH, and monthly atmospheric CO₂ concentration were explanatory factors, excluding interactions. Response and explanatory variables were normalized (mean = 0, SD = 1) to allow direct comparison of variables with disparate ranges of variation. Chlorophyll (Chl) was not sampled at PB-NERR and not available for many WA-DOE sites and therefore excluded from the full analysis. A supplementary analysis was conducted using the subset of 3123 observations with Chl. All mixed effects models were conducted with 'lmer' in R⁶⁴, and significance of fixed effects determined with likelihood ratio tests.

References

1. Aufdenkampe, A. K. *et al.* Riverine coupling of biogeochemical cycles between land, oceans, and atmosphere. *Front. Ecol. Environ.* **9**, 53–60 (2011).
2. Cloern, J. E. Our evolving conceptual model of the coastal eutrophication problem. *Mar. Ecol. Prog. Ser.* **210**, 223–253 (2001).
3. Orth, R. J. *et al.* A global crisis for seagrass ecosystems. *BioScience* **56**, 987–996 (2006).
4. Zu Ermgassen, P. S. E. *et al.* Historical ecology with real numbers: past and present extent and biomass of an imperilled estuarine habitat. *Proc. Biol. Sci.* **279**, 3393–3400 (2012).
5. Boyd, P. & Hutchins, D. Understanding the responses of ocean biota to a complex matrix of cumulative anthropogenic change. *Mar. Ecol. Prog. Ser.* **470**, 125–135 (2012).
6. Bauer, J. E. *et al.* The changing carbon cycle of the coastal ocean. *Nature* **504**, 61 (2013).
7. Kroeker, K., Kordas, R. L., Crim, R. N. & Singh, G. G. Meta-analysis reveals negative yet variable effects of ocean acidification on marine organisms. *Ecol. Lett.* **13**, 1419–1434 (2010).
8. Borges, A. V. & Gypens, N. Carbonate chemistry in the coastal zone responds more strongly to eutrophication than to ocean acidification. *Limnol. Oceanogr.* **55**, 346–353 (2010).
9. Page, H. N. *et al.* Differential modification of seawater carbonate chemistry by major coral reef benthic communities. *Coral Reefs* **35**, 1311–1325 (2016).
10. Baumann, H. & Smith, E. M. Quantifying metabolically driven pH and oxygen fluctuations in US nearshore habitats at diel to interannual time scales. *Estuaries Coasts*, <https://doi.org/10.1007/s12237-017-0321-3> (2017).

11. Gattuso, J.-P., Frankignoulle, M. & Wollast, R. Carbon and Carbonate Metabolism in Coastal Aquatic Ecosystems. *Annu. Rev. Ecol. Syst.* **29**, 405–434 (1998).
12. Cai, W.-J. Estuarine and coastal ocean carbon paradox: CO₂ sinks or sites of terrestrial carbon incineration? *Annu. Rev. Mar. Sci.* **3**, 123–145 (2011).
13. Martz, T. R., DeGrandpre, M. D., Strutton, P. G., McGillis, W. R. & Drennan, W. M. Sea surface pCO₂ and carbon export during the Labrador Sea spring-summer bloom: an *in situ* mass balance approach. *J. Geophys. Res.* **114**, C09008 (2009).
14. Jones, C. G., Lawton, J. H. & Shachak, M. Positive and negative effects of organisms as physical ecosystem engineers. *Ecology* **78**, 1946–1957 (1997).
15. Schindler, D. E., Carpenter, S. R., Cole, J. J., Kitchell, J. F. & Pace, M. L. Influence of food web structure on carbon exchange between lakes and the atmosphere. *Science* **277**, 248–251 (1997).
16. Silbiger, N. J. & Sorte, C. J. B. Biophysical feedbacks mediate carbonate chemistry in coastal ecosystems across spatiotemporal gradients. *Sci. Rep.* **8**, 796 (2018).
17. Pacella, S. R., Brown, C. A., Waldbusser, G. G., Labiosa, R. G. & Hales, B. Seagrass habitat metabolism increases short-term extremes and long-term offset of CO₂ under future ocean acidification. *Proc. Natl. Acad. Sci.* **115**, 3870 (2018).
18. Hofmann, G. E. *et al.* High-frequency dynamics of ocean pH: a multi-ecosystem comparison. *PLoS ONE* **6**, e28983 (2011).
19. Reum, J. C. P. *et al.* Interpretation and design of ocean acidification experiments in upwelling systems in the context of carbonate chemistry co-variation with temperature and oxygen. *ICES J. Mar. Sci.* **73**, 582–595 (2016).
20. Murray, C., Malvezzi, A., Gobler, C. & Baumann, H. Offspring sensitivity to ocean acidification changes seasonally in a coastal marine fish. *Mar. Ecol. Prog. Ser.* **504**, 1–11 (2014).
21. Pörtner, H. Integrating climate-related stressor effects on marine organisms: unifying principles linking molecule to ecosystem-level changes. *Mar. Ecol. Prog. Ser.* **470**, 273–290 (2012).
22. Cyronak, T. *et al.* Taking the metabolic pulse of the world's coral reefs. *PLOS ONE* **13**, e0190872 (2018).
23. Bates, N. R., Mathis, J. T. & Cooper, L. W. Ocean acidification and biologically induced seasonality of carbonate mineral saturation states in the western Arctic Ocean. *J. Geophys. Res. Oceans* **114**, n/a–n/a (2009).
24. Lowe, A. T., Roberts, E. A. & Galloway, A. W. E. Improved marine-derived POM availability and increased pH related to freshwater influence in an inland sea. *Limnol. Oceanogr.*, <https://doi.org/10.1002/lno.10357> (2016).
25. Caffrey, J. M. Production, respiration, and net ecosystem metabolism in U.S. estuaries. *Environ. Monit. Assess.* **81**, 207–219 (2003).
26. Wootton, J. T., Pfister, C. A. & Forester, J. D. Dynamic patterns and ecological impacts of declining ocean pH in a high-resolution multi-year dataset. *Proc. Natl. Acad. Sci. USA* **105**, 18848–18853 (2008).
27. Duarte, C. M. *et al.* Is Ocean Acidification an Open-Ocean Syndrome? Understanding Anthropogenic Impacts on Seawater pH. *Estuaries Coasts* **36**, 221–236 (2013).
28. Provoost, P., van Heuven, S., Soetaert, K., Laane, R. W. P. M. & Middelburg, J. J. Seasonal and long-term changes in pH in the Dutch coastal zone. *Biogeosciences* **7**, 3869–3878 (2010).
29. Dore, J. E., Lukas, R., Salder, D. W., Church, M. J. & Karl, D. M. Physical and biogeochemical modulation of ocean acidification in the central North Pacific. *Proc. Natl. Acad. Sci. USA* **106**, 12235–12240 (2009).
30. Ruesink, J., Yang, S. & Alan C. Trimble. Variability in carbon availability and Eelgrass (*Zostera marina*) biometrics along an estuarine gradient in Willapa Bay, WA, USA. *Estuaries Coasts* 1–10, <https://doi.org/10.1007/s12237-014-9933-z> (2015).
31. Breitburg, D. L. *et al.* And on Top of All That... Coping with ocean acidification in the midst of many stressors. *Oceanography* **28**, 48–61 (2015).
32. Yang, H., Sturmer, L. N. & Baker, S. FA191: Molluscan shellfish aquaculture and production (2015).
33. Barton, A., Hales, B., Waldbusser, G. G., Langdon, C. & Feely, R. A. The Pacific oyster, *Crassostrea gigas*, shows negative correlation to naturally elevated carbon dioxide levels: Implications for near-term ocean acidification effects. *Limnol. Oceanogr.* **57** (2012).
34. Bates, N. R. *et al.* A time-series view of changing ocean chemistry due to ocean uptake of anthropogenic CO₂ and ocean acidification. *Oceanography* **27**, 126–141 (2014).
35. Kapsenberg, L., Alliouane, S., Gazeau, F., Mousseau, L. & Gattuso, J.-P. Coastal ocean acidification and increasing total alkalinity in the northwestern Mediterranean Sea. *Ocean Sci.* **13**, 411–426 (2017).
36. Waldbusser, G. G. *et al.* Saturation-state sensitivity of marine bivalve larvae to ocean acidification. *Nat. Clim Change* **5**, 273–280 (2015).
37. McLaskey, A. *et al.* Development of *Euphausia pacifica* (krill) larvae is impaired under pCO₂ levels currently observed in the Northeast Pacific. *Mar. Ecol. Prog. Ser.* **555**, 65–78 (2016).
38. Starr, M., Himmelman, J. H. & Therriault, J.-C. Coupling of nauplii release in barnacles with phytoplankton blooms: a parallel strategy to that of spawning in urchins and mussels. *J. Plankton Res.* **13**, 561–571 (1991).
39. Wahl, M. *et al.* Macroalgae may mitigate ocean acidification effects on mussel calcification by increasing pH and its fluctuations. *Limnol. Oceanogr.* **63**, 3–21 (2018).
40. Koweeck, D. A. *et al.* A year in the life of a central California kelp forest: physical and biological insights into biogeochemical variability. *Biogeosciences* **14**, 31–44 (2017).
41. Kapsenberg, L. & Hofmann, G. E. Ocean pH time-series and drivers of variability along the northern Channel Islands, California, USA. *Limnol. Oceanogr.* **61**, 953–968 (2016).
42. Pelletier, G., Roberts, M., Keyzers, M. & Alin, S. R. Seasonal variation in aragonite saturation in surface waters of Puget Sound - a pilot study. *Elem. Sci. Anthr.* **6**, 5 (2018).
43. Hu, X., Cai, W.-J., Rabalais, N. N. & Xue, J. Coupled oxygen and dissolved inorganic carbon dynamics in coastal ocean and its use as a potential indicator for detecting water column oil degradation. *Gulf Mex. Ecosyst. - Macondo Blowout* **129**, 311–318 (2016).
44. Hauri, C. *et al.* Two decades of inorganic carbon dynamics along the West Antarctic Peninsula. *Biogeosciences* **12**, 6761–6779 (2015).
45. Dinauer, A. & Mucci, A. Spatial variability in surface-water pCO₂ and gas exchange in the world's largest semi-enclosed estuarine system: St. Lawrence Estuary (Canada). *Biogeosciences* **14**, 3221–3237 (2017).
46. Kim, D., Park, G.-H., Baek, S. H., Choi, Y. & Kim, T.-W. Physical and biological control of aragonite saturation in the coastal waters of southern South Korea under the influence of freshwater. *Mar. Pollut. Bull.* **129**, 318–328 (2018).
47. Yeakel, K. L. *et al.* Shifts in coral reef biogeochemistry and resulting acidification linked to offshore productivity. *Proc. Natl. Acad. Sci.* **112**, 14512 (2015).
48. Vargas, C. A. *et al.* Influences of riverine and upwelling waters on the coastal carbonate system off Central Chile, and their ocean acidification implications: Carbonate system in the coastal ocean. *J. Geophys. Res. Biogeosciences*, <https://doi.org/10.1002/2015JG003213> (2016).
49. Feely, R. A. *et al.* The combined effects of ocean acidification, mixing, and respiration on pH and carbonate saturation in an urbanized estuary. *Estuar Coast Shelf Sci* **88** (2010).
50. Orr, J. C. *et al.* Anthropogenic ocean acidification over the twenty-first century and its impact on calcifying organisms. *Nature* **437**, 681–686 (2005).
51. Wissel, B., Quiñones-Rivera, Z. J. & Fry, B. Combined analyses of O₂ and CO₂ for studying the coupling of photosynthesis and respiration in aquatic systems. *Can. J. Fish. Aquat. Sci.* **65**, 2378–2388 (2008).
52. Ianson, D., Allen, S. E., Moore-Maley, B. L., Johannessen, S. C. & Macdonald, R. W. Vulnerability of a semienclosed estuarine sea to ocean acidification in contrast with hypoxia. *Geophys. Res. Lett.* **43**, 5793–5801 (2016).
53. Borges, A. & Abril, G. Carbon dioxide and methane dynamics in estuaries. *Treatise Estuar. Coast. Sci. Vol. 5 Biogeochem.* 119–161 (2011).

54. Welti, N. *et al.* Bridging Food Webs, Ecosystem Metabolism, and Biogeochemistry Using Ecological Stoichiometry Theory. *Front. Microbiol.* **8**, 1298 (2017).
55. Borges, A. V., Delille, B. & Frankignoulle, M. Budgeting sinks and sources of CO₂ in the coastal ocean: Diversity of ecosystems counts. *Geophys. Res. Lett.* **32**, n/a–n/a (2005).
56. Baumann, H., Wallace, R. B., Tagliaferri, T. & Gobler, C. J. Large natural pH, CO₂ and O₂ fluctuations in a temperate tidal salt marsh on diel, seasonal, and interannual time scales. *In Estuar Coasts* (2014).
57. Wallace, R. B., Baumann, H., Grear, J. S., Aller, R. C. & Gobler, C. J. Coastal ocean acidification: The other eutrophication problem. *Estuar. Coast. Shelf Sci.* **148**, 1–13 (2014).
58. Bos, J., Krembs, C. & Albertson, S. Quality assurance for long-term marine water column pH data (2016).
59. Gattuso, J. -P. *et al.* 'seacarb': Seawater carbonate chemistry in R (2015).
60. Fassbender, A. J. *et al.* Estimating total alkalinity in the Washington State coastal zone: complexities and surprising utility for ocean acidification research. *Estuaries Coasts* **40**, 404–418 (2017).
61. Murray, J. W. *et al.* An inland sea high nitrate-low chlorophyll (HNLC) region with naturally high pCO₂. *Limnol. Oceanogr.* **60**, 957–966 (2015).
62. Sarmiento, J. L. & Gruber, N. *Ocean biogeochemical dynamics*. (Princeton University Press, 2006).
63. Zuur, A. F., Ieno, E. N., Walker, N., Saveliev, A. A. & Smith, G. M. *Mixed effects models and extensions in ecology with R*. (Springer, 2009).
64. Bates, D., Maechler, M., Bolker, B. & Walker, S. Fitting Linear Mixed-Effects Models Using lme4. *J. Stat. Softw.* **67**, 1–48 (2015).

Acknowledgements

We would like to thank K. Cogert, C. Crifo, J. Hsiao, D.E. Schindler, and P. Quay for feedback on the manuscript. M. Horwith, L. Comte, P. Matson, and the WA Department of Ecology Ocean Acidification modeling team provided valuable feedback on analyses.

Author Contributions

A.T.L. and J.R. conceived of research, J.B. collected data, A.T.L. and J.B. analyzed data, A.T.L. wrote the manuscript. All authors reviewed the manuscript.

Additional Information

Supplementary information accompanies this paper at <https://doi.org/10.1038/s41598-018-37764-4>.

Competing Interests: The authors declare no competing interests.

Publisher's note: Springer Nature remains neutral with regard to jurisdictional claims in published maps and institutional affiliations.



Open Access This article is licensed under a Creative Commons Attribution 4.0 International License, which permits use, sharing, adaptation, distribution and reproduction in any medium or format, as long as you give appropriate credit to the original author(s) and the source, provide a link to the Creative Commons license, and indicate if changes were made. The images or other third party material in this article are included in the article's Creative Commons license, unless indicated otherwise in a credit line to the material. If material is not included in the article's Creative Commons license and your intended use is not permitted by statutory regulation or exceeds the permitted use, you will need to obtain permission directly from the copyright holder. To view a copy of this license, visit <http://creativecommons.org/licenses/by/4.0/>.

© The Author(s) 2019